



Conductivity and Viscosity of PC-DEC and PC-EC Solutions of LiPF₆

Michael S. Ding*^z and T. Richard Jow*

Army Research Laboratory, Adelphi, Maryland 20783, USA

Conductivity κ and viscosity η of propylene carbonate (PC)-diethyl carbonate (DEC) and PC-ethylene carbonate (EC) solutions of LiPF₆ were experimentally determined, the former at salt molalities m from 0.2 to 2.4 mol kg⁻¹, solvent compositions w from 0 to 0.7 weight fraction of DEC and 0 to 0.6 weight fraction of EC, and temperatures θ from 60 to -80°C, the latter indirectly and qualitatively through measuring the glass transition temperature T_g in the same ranges of m and w . The T_g increased with m , and decreased with w of DEC but increased with w of EC, indicating a concurrent change in the η of the solutions. The κ of the PC-DEC solution of LiPF₆ peaked in both m and w thus forming a dome in its 3D presentation in the mw coordinates, while that of the PC-EC solution peaked only in m resulting in an arch-shaped surface. As θ lowered, these κ surfaces fell in height and shifted in the direction of low η . These observations correlated well with the changes of dielectric constant ϵ and viscosity η of the solutions with the same set of variables. More detailed study of the effects of DEC and EC on the κ of PC solution of LiPF₆ demonstrated the benefit of having a low- η solvent component in an electrolyte for it to have a decent κ at low θ and the independence on θ of ion association in these solutions in support of an earlier finding. The κ - T data of the PC-DEC solution of LiPF₆ were fit with the Vogel-Tamman-Fulcher equation for an evaluation of its apparent activation energy E_a and its vanishing mobility temperature T_0 , the former shown to be a simple surface in the mw coordinates slanting up in the direction of high η , and the latter another one slanting up in the same direction and lying beneath the surface of T_g by more than ten degrees.
© 2003 The Electrochemical Society. [DOI: 10.1149/1.1566019] All rights reserved.

Manuscript submitted July 17, 2002; revised manuscript received November 14, 2002. Available electronically March 27, 2003.

The aim of this study is to provide a relatively complete picture for the change of conductivity κ of propylene carbonate (PC)-diethyl carbonate (DEC) and PC-ethylene carbonate (EC) solutions of LiPF₆ with their salt molality m and solvent weight fraction w at different temperatures θ . (θ denotes temperature in °C, and T in K.¹) It is also to establish a firm correlation of this change of κ with the changes of dielectric constant ϵ and viscosity η of the solutions with the same set of variables and thereby providing some directions for the formulation of electrolytes with desired properties. This study, together with a parallel study of PC-DEC and PC-EC solutions of LiBF₄ currently in review² and an earlier one on the ϵ and η of PC-DEC and PC-EC solvents,³ is expected to shed considerable light on how and why LiPF₆ and LiBF₄ behave differently in organic solvents and on the mechanisms by which their behavior is affected and can thus be controlled by the changes of m , w , and θ .

Electrolytic conductivity is the most important and fundamental property of an electrolyte. Its value is determined by the number of conducting ions in the electrolyte solution, which we denote as the effective molality m_e , the charge number of the ions, which we assume to be unity as we consider only univalent ions here, and the mobility u with which the ions move in response to an applied electric field. The m_e and u in turn are largely determined by the properties ϵ and η of the electrolyte which are more amenable to measurement and control. For an electrolyte of the form salt _{m} -solvent _{$1-w$} -cosolvent _{w} , its thermodynamic state, and along with its ϵ and η , is uniquely determined when we fix its m , w , and θ and subject it to no pressure other than the room pressure. As such, its effective molality m_e is the nominal molality m subtracted by a fraction due to ion association which rises with smaller ϵ and higher m , and the mobility u of its ions is determined largely by η in a reciprocal manner. It is therefore critically important to determine the dependency of ϵ and η on m , w , and θ if one hopes to understand the mechanisms through which κ is affected and can therefore be controlled through the changes in these common variables.

For this reason, the ϵ and η of many solvents and electrolytes have been measured as functions of m or w , as well as κ of many electrolytes. In particular, in connection to this study, ϵ of PC-DEC

and PC-EC solvents has been systematically measured as a function of w and θ , from which Bjerrum critical distance for ion association has been determined and found to be almost independent of θ . The η of the solvents has also been estimated by measuring their glass transition temperature T_g and found to fall with weight fraction w of DEC and to rise with w of EC.³ The choice of these two solvents for the current study was due to their wide variation in ϵ and in the nature of the solvents and due to the low melting points of PC and DEC and the strong resistance of PC to crystallization. The reason for choosing LiPF₆ as the subject salt was more obvious: it is the most popular lithium salt for battery applications and one of the very few viable ones so far available. As such, a relatively complete and reliable set of data for these electrolyte systems would be useful not only in terms of practical applications but also as a baseline for future comparison with other electrolytes of lithium salts and organic solvents.

Experimental

Sample preparation.—PC of 99.98% purity and DEC and EC both of 99.95% were purchased from Grant Chemical, and LiPF₆ of 99.9% from Stella Chemifa. In an argon-filled dry box, PC and DEC were mixed to form seven mixtures, in addition to pure PC, in weight fractions (w) of DEC from 0.1 to 0.7 in 0.1 increment, and PC and EC were made into four mixtures with w of EC from 0.15 to 0.6 in 0.15 increment, from which 12 electrolytes were subsequently made by dissolving LiPF₆ into each of the solvents to a molality (m) of around 2.4 mol kg⁻¹. Conductivity measurement on these solutions and their subsequent dilution for the next set of less concentrated solutions were done in a dry room. At the end of each measurement, a small amount of sample was taken from each electrolyte for determination of its glass transition temperature.^{4,5}

Measurement of glass transition temperature.—A modulated differential scanning calorimeter (MDSC 2920, TA Instruments) cooled with liquid nitrogen was used to determine the glass transition temperature T_g of a sample. Its temperature scale was calibrated with n -hexane (melting point 177.84 K) and n -decane (243.51 K). Vitri-fication of the sample was achieved by dipping into liquid nitrogen a small amount of sample crimp-sealed in a pair of aluminum pan and lid (0219-0062, Perkin Elmer Instruments). The sample was then quickly placed on the DSC sample stage that had been kept at a temperature below T_g of the sample. A modulated heating schedule

* Electrochemical Society Active Member.

^z E-mail: mding@arl.army.mil

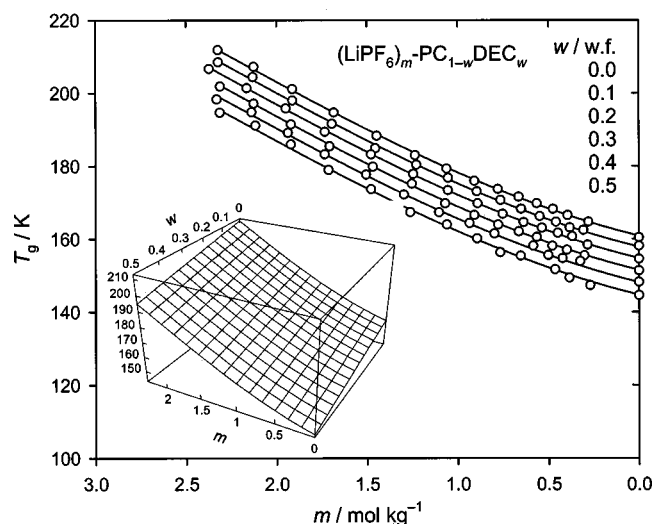


Figure 1. Change of glass transition temperature T_g with salt molality m and solvent weight fraction w for $(\text{LiPF}_6)_m\text{-PC}_{1-w}\text{DEC}_w$ solution. (○) represent the measured data and the curves plot their fitting function of Eq. 1, which is also plotted as a 3D surface in the inset figure.

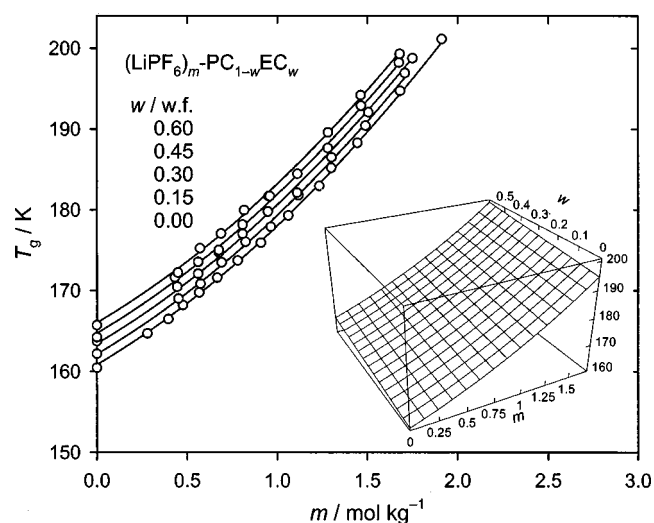


Figure 2. Change of T_g with m and w for $(\text{LiPF}_6)_m\text{-PC}_{1-w}\text{EC}_w$ solution. (○) represent the measured data and the curves plot their fitting function of Eq. 2, which is also plotted as a 3D surface in the inset figure.

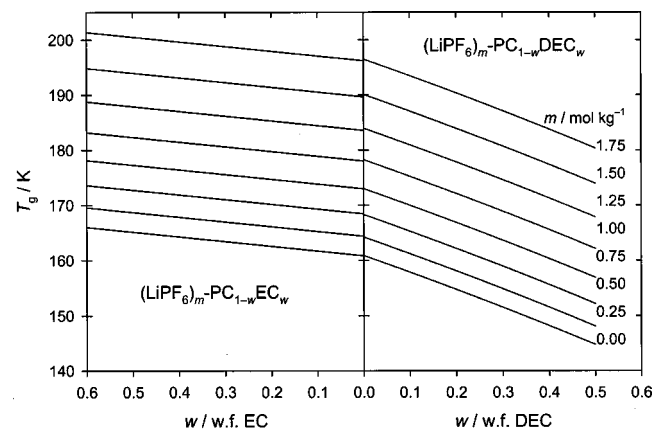


Figure 3. Comparison of the changes in T_g with w at different salt molalities m for $(\text{LiPF}_6)_m\text{-PC}_{1-w}\text{DEC}_w$ and $(\text{LiPF}_6)_m\text{-PC}_{1-w}\text{EC}_w$ solutions, according to Eq. 1 and 2.

Table I. Fitted values for the parameters of the fitting equation as written in the table for $(\text{LiPF}_6)_m\text{-PC}_{1-w}\text{DEC}_w$ solution, with κ in the unit of $\mu\text{S cm}^{-1}$, application limits of 0.2 to 2.4 mol kg^{-1} for m and 0 to 0.7 weight fraction of DEC for w , and e_f as the fitting error in percent of the range of the data.

$\ln \kappa = (a_0 + a_1w + a_2w^2 + a_3w^3) \ln m + (b_0 + b_1w + b_2w^2 + b_3w^3)m + (c_0 + c_1w + c_2w^2 + c_3w^3)m^2 + (d_0 + d_1w + d_2w^2 + d_3w^3)m^3$	θ (°C)	a_0	a_1	a_2	a_3	b_0	b_1	b_2	b_3	c_0	c_1	c_2	c_3	d_0	d_1	d_2	d_3	e_f
59.0	0.98266	0.0019017	-0.77917	0.73708	10.544	0.12973	-0.72595	-1.0757	-1.0965	0.41426	0.16164	0.45434	-0.04759	-0.030067	0.091892	-0.14765	0.87	
49.2	0.98026	0.010715	-0.88543	0.86368	10.408	0.20798	-0.96082	-0.79542	-1.1086	0.34609	0.60897	-0.00371	-0.07647	0.025577	-0.054694	-0.017733	0.80	
39.3	0.97155	-0.021157	-0.73722	0.71525	10.242	0.21042	-0.69656	-1.0508	-1.1066	0.45527	0.1971	0.39499	-0.11704	0.035775	0.044802	-0.12873	0.67	
29.4	0.96513	-0.32885	0.31534	-0.16204	10.062	-0.27977	1.2361	-2.6678	-1.1116	1.178	-2.2913	2.4998	-0.16674	-0.076974	0.61021	-0.6288	0.74	
19.5	0.94617	0.11993	-0.8465	0.6275	9.839	0.59345	-0.81433	-1.2722	-1.096	0.18739	0.25399	0.79399	-0.23324	0.20628	0.053896	-0.28106	0.63	
9.7	0.9092	0.43559	-1.5143	1.0239	9.522	1.1855	-1.7604	-0.77533	-1.0372	-0.43401	1.368	0.26661	-0.33017	0.42693	-0.14722	-0.24481	0.65	
-0.2	0.86877	0.059019	-0.15606	-0.042389	9.2087	0.75066	0.444	-2.5819	-0.94605	0.22384	-1.4437	2.6135	-0.46715	0.41806	0.48371	-0.82903	0.63	
-10.0	0.77765	0.27149	-0.22396	-0.16579	8.7248	1.281	0.45538	-2.9705	-0.73267	-0.20005	-1.838	3.4286	-0.67065	0.61783	0.81207	-1.2643	0.58	
-19.8	0.71073	-0.33769	1.9176	-1.8429	8.229	0.25682	4.758	-6.3935	-0.60254	1.6673	-8.3378	8.5113	-0.89669	0.25298	2.7322	-2.7988	0.50	
-29.5	0.66511	-0.78304	3.3101	-2.9121	7.699	-0.33197	7.3982	-8.4847	-0.56557	3.0772	-12.495	11.6	-1.142	0.0034092	4.0557	-3.7685	0.41	
-39.4	0.61459	-0.97381	3.6376	-3.0017	7.0507	-0.42616	8.1945	-8.8627	-0.58359	4.1674	-14.355	12.306	-1.4335	-0.20135	4.9178	-4.1682	0.40	

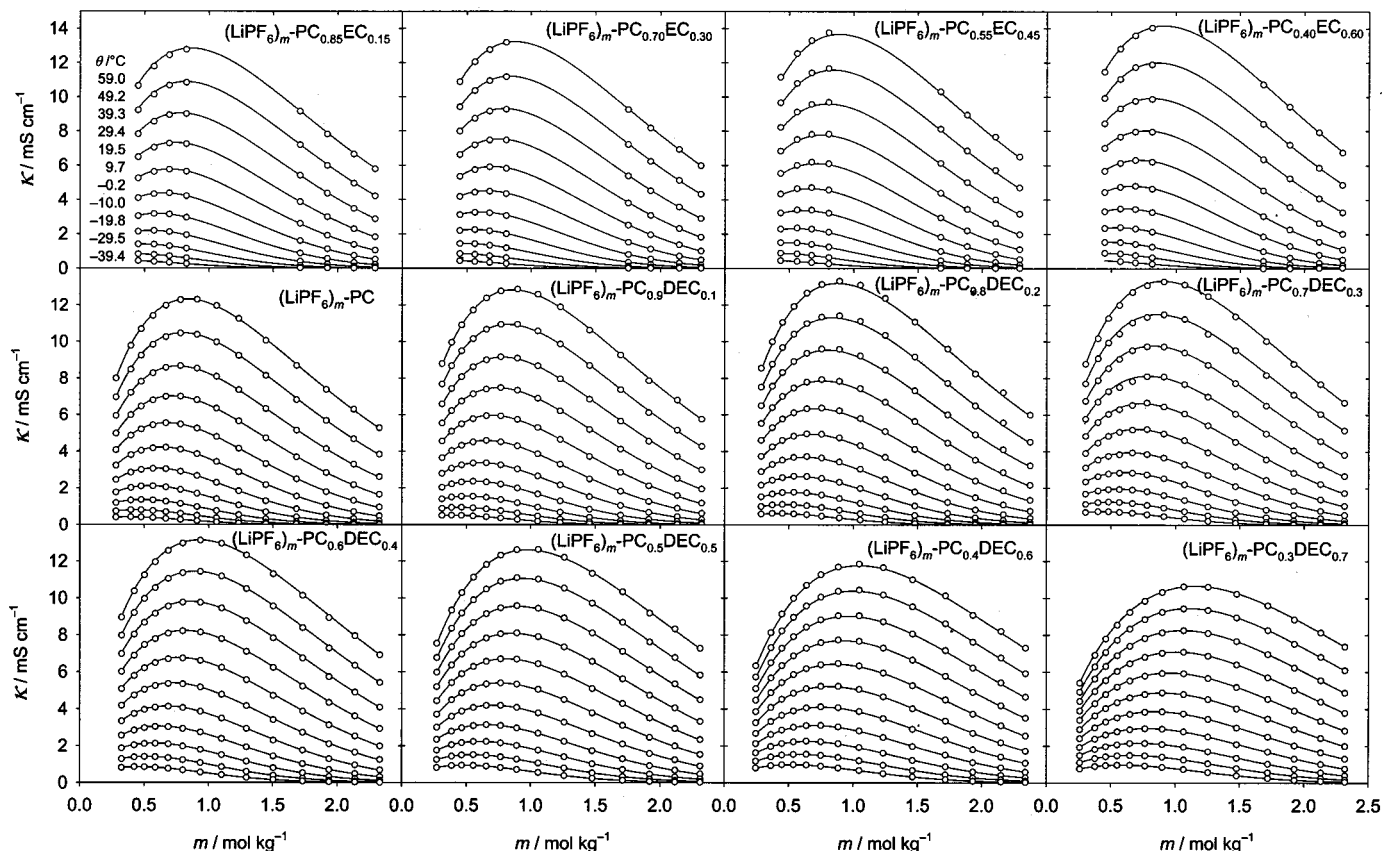


Figure 4. Change of conductivity κ with salt molality m at different temperatures θ and solvent weight fractions w for $(\text{LiPF}_6)_m\text{-PC}_{1-w}\text{-DEC}_w$ and $(\text{LiPF}_6)_m\text{-PC}_{1-w}\text{-EC}_w$ solutions. (○) represent measured data and the curves plot their fitting functions listed in Tables I and II.

was then applied, with a heating rate of $2^\circ\text{C}/\text{min}$ and a modulation of 60 s period and 0.5° amplitude. T_g of the sample was subsequently determined on the reversing component of the heat flow at the inflection point of the endothermic step associated with the glass transition.⁴

Measurement of electrolytic conductivity.—Conductivity κ of the electrolytes was measured with an HP (now Agilent) 4284A precision LCR meter at selected temperatures within a Tenney Jr. environmental chamber, controlled and coordinated with a house-made computer program. The conductivity cells consisted of a pair of platinum-iridium electrodes and a Pyrex cell body that could be sealed with a ground-glass stopper. The cell constants were calibrated with a standard KCl solution to be approximately 0.1 cm^{-1} . Temperature θ of the measurements went from 60 to -80°C in 10°C decrement, stopping at each for an hour of thermal equilibration before a measurement. The measurement consisted of an impedance scan from 1 MHz to 20 Hz with an amplitude of 10 mV , from which a Z''/Z' plot was made and κ was evaluated from the impedance curve. Precision of the measurement was determined to be 0.04% from 32 replicate measurements on the standard solution at 15°C under actual measurement conditions. Inaccuracy of the measurement was considered for three sources: weighing error in sample preparation, temperature variation of the cell constants, and uncertainty in the sample temperature during measurement. The weighing error inaccuracy was estimated to be no more than 0.02% after taking into account the cumulative effect of the successive sample dilutions. Errors due to the temperature variation of the cell constants were estimated to be less than 0.2% in κ . For the actual temperatures of the samples during a measurement, they were recorded independently with a set of five thermocouples placed next to the sample cells, which stabilized at a temperature slightly off the

set temperature, with a temporal distribution of 0.05° and a spatial distribution of 0.2° . The error in κ due to these temperature distributions was estimated to be no more than 0.3% . The overall inaccuracy in the measurement of κ was therefore estimated to be 0.5% , which should be considered the upper limit of error in every measured value of κ in this work.

Results and Discussion

Dielectric constants ϵ of the binary solvents $\text{PC}_{1-w}\text{-DEC}_w$ and $\text{PC}_{1-w}\text{-EC}_w$ have been systematically measured and found to change monotonically and smoothly with w and θ , falling with θ universally and falling with w in $\text{PC}_{1-w}\text{-DEC}_w$ but rising in $\text{PC}_{1-w}\text{-EC}_w$ ³ (ϵ of DEC, PC, and EC at 40°C : 2.809, 61.43, and 89.78^{6,7}), as has been observed in many other similar solvent mixtures.^{4,8-11} From these results, Bjerrum critical distance was calculated for univalent ions, which indicated that ion pairing should be nearly independent of θ , rising only slightly with θ for high- ϵ solvents such as EC-rich mixtures of PC-EC and falling slightly for low- ϵ solvents such as DEC-rich mixtures of PC-DEC. But it showed a strong dependency on w , rising steadily as ϵ fell with the change of w . Viscosity η of the two solvents has also been studied indirectly by measuring their T_g , whose connection with η was argued and demonstrated to be a qualitative but definite one: a higher T_g was associated with a higher η for similar liquids.³ With this association, η of the solvents fell steadily with w in $\text{PC}_{1-w}\text{-DEC}_w$ but rose in $\text{PC}_{1-w}\text{-EC}_w$, as expected.^{4,8-10,12} These changes also indicated that while DEC had a considerably lower η than PC, η of EC was not much higher than that of PC, consistent with the published values (η of DEC, PC, and EC at 40°C : 0.622, 1.91, and 1.93 mPa s^{6,7}).

Table II. Fitted values for the parameters of the fitting equation as written in the table for $(\text{LiPF}_6)_m\text{-PC}_{1-w}\text{EC}_w$ solution, with κ in the unit of $\mu\text{S cm}^{-1}$, application limits of 0.4 to 2.3 mol kg^{-1} for m and 0 to 0.6 weight fraction of EC for w , and e_f as the fitting error in percent of the range of the fitting data.

$\ln \kappa = (a_0 + a_1w + a_2w^2) \ln m + (b_0 + b_1w + b_2w^2)m + (c_0 + c_1w + c_2w^2)w + (d_0 + d_1w + d_2w^2)m^2$	a_0	a_1	a_2	b_0	b_1	b_2	c_0	c_1	c_2	d_0	d_1	d_2	e_f
59.0	0.95436	0.36113	-0.66932	10.5	0.56617	-0.93488	-1.0192	-0.48197	1.2511	-0.063341	0.09755	-0.24031	0.98
49.2	0.95507	0.252	-0.39412	10.371	0.37105	-0.45805	-1.0397	-0.21886	0.63476	-0.089643	0.028536	-0.097063	0.88
39.3	0.94319	0.32924	-0.68078	10.199	0.50135	-0.93193	-1.0294	-0.35609	1.2147	-0.13202	0.047604	-0.21897	0.79
29.4	0.92831	0.22541	-0.58339	10.002	0.33242	-0.77613	-1.0143	-0.11191	1.0043	-0.1861	-0.014982	-0.17749	0.73
19.5	0.91893	0.0092963	-0.38704	9.7944	-0.043633	-0.43917	-1.0173	0.40251	0.57476	-0.24927	-0.14263	-0.092836	0.71
9.7	0.89481	-0.21634	-0.20465	9.5273	-0.41921	-0.14672	-0.98665	0.95625	0.15934	-0.33921	-0.28213	-0.015613	0.69
-0.2	0.84351	-0.59259	0.32691	9.1653	-1.0439	0.73703	-0.87704	1.8444	-1.0398	-0.4798	-0.51145	0.24716	0.65
-10.0	0.76557	-0.29811	-0.14235	8.7006	-0.46484	-0.17285	-0.6904	1.1025	0.18731	-0.68073	-0.34134	-0.097549	0.59
-19.8	0.68812	-1.2392	1.5149	8.1768	-2.0771	2.6602	-0.5254	3.4045	-3.7159	-0.91977	-0.98679	0.86871	0.58
-29.5	0.63199	-1.4964	1.9855	7.6156	-2.5166	3.4225	-0.44811	4.2247	-4.9065	-1.1865	-1.3649	1.2215	0.61
-39.4	0.57091	-1.0025	-0.88852	6.9251	-1.643	-1.5462	-0.40586	3.1628	1.918	-1.5177	-1.1058	-0.80403	0.71

Change of viscosity with salt content and solvent composition.—PC-DEC solution of LiPF_6 .—Figure 1 plots the results of measurement of T_g for $(\text{LiPF}_6)_m\text{-PC}_{1-w}\text{DEC}_w$ solution, with the open circles for the measured data and the curves for their fitting function

$$T_g = 160.89 + 11.849m + 6.4258m^2 - 0.89805m^3 - 29.785w - 4.9844w^2 \quad [1]$$

where T_g is in kelvin, the application limits are 0 to 2.4 mol kg^{-1} for m and 0 to 0.5 weight fraction for w , and the fitting error is 0.72% of the range of the fitting data. This equation is also plotted as a T_g surface in the mw coordinates as inset in the figure, describing a simple surface slanting down from the high- η corner of high m and low w toward the low- η corner of low m and high w . It is thus clear that the addition of LiPF_6 in $\text{PC}_{1-w}\text{DEC}_w$ solvent continuously raised η of the resulting solution, a phenomenon observed in many other electrolytes.^{4,9,10,13,14} It also seems that the rise of T_g due to the addition of salt was independent of that due to the change of solvent composition. This can be seen in the shape of the T_g surface and the curves and above all in the absence of a cross-product term in the fitting function of Eq. 1. It is likely that the effects of w and of m on the η of the solutions were also independent of each other.

PC-EC solution of LiPF_6 .—Results of the T_g measurement on $(\text{LiPF}_6)_m\text{-PC}_{1-w}\text{EC}_w$ solution are plotted in Fig. 2. Apart from T_g rising with w instead of falling, this electrolyte system has the same pattern of change in T_g with m and w as that shown in Fig. 1 for $(\text{LiPF}_6)_m\text{-PC}_{1-w}\text{DEC}_w$, with T_g tracing out a surface slanting down from the high- η corner of high m and w toward the low- η corner of low m and w . And as before, the effects of m and w on η seemed independent of each other, as suggested by the absence of a cross-product term in the fitting function to the T_g data of $(\text{LiPF}_6)_m\text{-PC}_{1-w}\text{EC}_w$

$$T_g = 160.83 + 13.178m + 4.0151m^2 + 8.646w \quad [2]$$

This equation has as its application limits 0 to 1.7 mol kg^{-1} for m and 0 to 0.6 weight fraction for w and carries a fitting error of 1.0% of the range of the fitting data.

Comparison of the PC-DEC and PC-EC solutions.—To compare the changes of η for the two solutions, Eq. 1 and 2 are plotted together in Fig. 3 with T_g as a function of w at different salt molalities. As shown, the pattern of T_g - w curve found for the two solvents³ is preserved in adding the salt, the curves with different values of m differing with one another only by a constant value. That this holds true in such a wide range of w across the two solvent systems seems to indicate that the mechanism by which the addition of a salt raises the η of a solvent is independent of the nature of the solvent molecules. An implication of this observation is that the difference in η between a pair of different electrolytes is about the same as that between their solvents as long as they have the same salt at the same molality.

Change of conductivity with salt content, solvent composition, and temperature.—PC-DEC solution of LiPF_6 .—With the estimation of the change of η with m and w for $(\text{LiPF}_6)_m\text{-PC}_{1-w}\text{DEC}_w$ and $(\text{LiPF}_6)_m\text{-PC}_{1-w}\text{EC}_w$ solutions and the evaluation of the change of ε for $\text{PC}_{1-w}\text{DEC}_w$ and $\text{PC}_{1-w}\text{EC}_w$ solvents, we now turn to the κ of the solutions. Results of the κ measurement between 60 and -40°C for the two solutions are plotted in Fig. 4 as 12κ - m plots, one for each solvent composition. The open circles represent the measured data and the curves plot their fitting functions $\kappa = f(m, w)$ at the particular temperatures. These functions were obtained by extending the Casteel-Amis equation¹⁵ to include w as an additional variable by setting the equation parameters to polynomial functions of w . That is

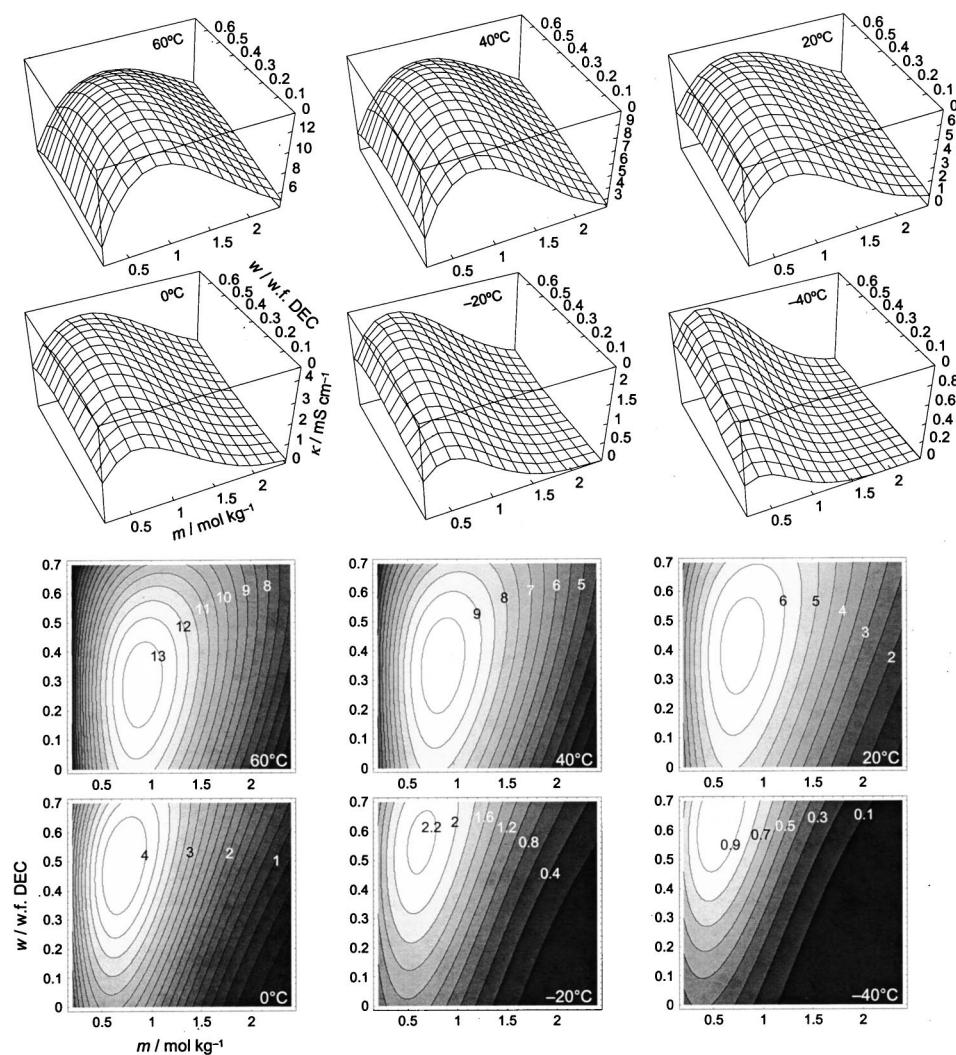


Figure 5. Change of conductivity κ with simultaneous changes in salt molarity m and solvent weight fraction w for $(\text{LiPF}_6)_m\text{-PC}_{1-w}\text{DEC}_w$ solution according to the fitting functions listed in Table I. Each function is doubly represented by a surface plot (upper plots) and a contour plot (lower plots) with the set temperature and the contour values indicated in the plots.

$$\kappa = m^a \exp(b + cm + dm^2) \quad [3]$$

where a , b , c , and d are third-degree polynomials of w for $(\text{LiPF}_6)_m\text{-PC}_{1-w}\text{DEC}_w$

$$p = p_0 + p_1w + p_2w^2 + p_3w^3 \quad [4]$$

and second-degree polynomials of w for $(\text{LiPF}_6)_m\text{-PC}_{1-w}\text{EC}_w$

$$p = p_0 + p_1w + p_2w^2 \quad [5]$$

where p in Eq. 4 and 5 stands for a , b , c , or d . Use of Eq. 3 as the basic form for the fitting functions was due to its ability to faithfully describe the dependency of κ on m in wide ranges of m as shown in Fig. 4, which was difficult to achieve with a polynomial function. The choice for the degrees of the polynomials of Eq. 4 and 5, was based on their use in Eq. 3 resulting in the best fit to the measured data. Also, search for an all-inclusive function $\kappa = f(m, w, \theta)$ was attempted by including θ as an additional variable in Eq. 4 and 5 in fitting, resulting in functions that were satisfactory only in limited ranges of the variables. Thus, the bivariate function of Eq. 3 was fitted to the $\kappa(m, w)$ data for each θ for the determination of the parameters, with the results listed in Table I for $(\text{LiPF}_6)_m\text{-PC}_{1-w}\text{DEC}_w$ solution and in Table II for $(\text{LiPF}_6)_m\text{-PC}_{1-w}\text{EC}_w$. The high accuracy with which these functions describe their fitting data can be seen in the fitting errors listed in the tables and in Fig. 4 where the functions are plotted together

with their fitting data. These functions, in addition to being a succinct and accurate summary of the measured data, provide an invaluable means for observing the change of κ with simultaneous changes of w and m at different temperatures.

The data of $(\text{LiPF}_6)_m\text{-PC}$ electrolytes, as shown in one of the Fig. 4 plots, served as an end member in both $(\text{LiPF}_6)_m\text{-PC}_{1-w}\text{DEC}_w$ and $(\text{LiPF}_6)_m\text{-PC}_{1-w}\text{EC}_w$ solutions with respect to the variation of w , and as such, were used in fitting Eq. 3 for both systems. Also, the absence of some experimental data for the latter solution in the top-row plots was due to a momentary malfunctioning of the temperature control of the environmental chamber. Because this malfunctioning had no effect on the preparations of the electrolyte samples, and the Casteel-Amis equation described the κ - m data accurately for many electrolyte systems such as PC-DEC solution of LiPF_6 (Fig. 4) and others,^{13,15-18} the remaining data for which proper control of θ was maintained were fitted with Eq. 3 and 5, resulting in fitting functions that described the measured data satisfactorily, as listed in Table II and plotted in Fig. 4.

To observe the change of κ with simultaneous changes of m and w for $(\text{LiPF}_6)_m\text{-PC}_{1-w}\text{DEC}_w$ solution, the fitting functions of Table I are plotted in Fig. 5 for temperatures from 60 to -40°C in 20°C decrement, once as a surface plot and once as a contour plot for each. The most conspicuous feature emerging from these plots is the "dome" shape of the κ surfaces, as a result of κ peaking in both m and w . Peaking of κ in m is a common feature for liquid electro-

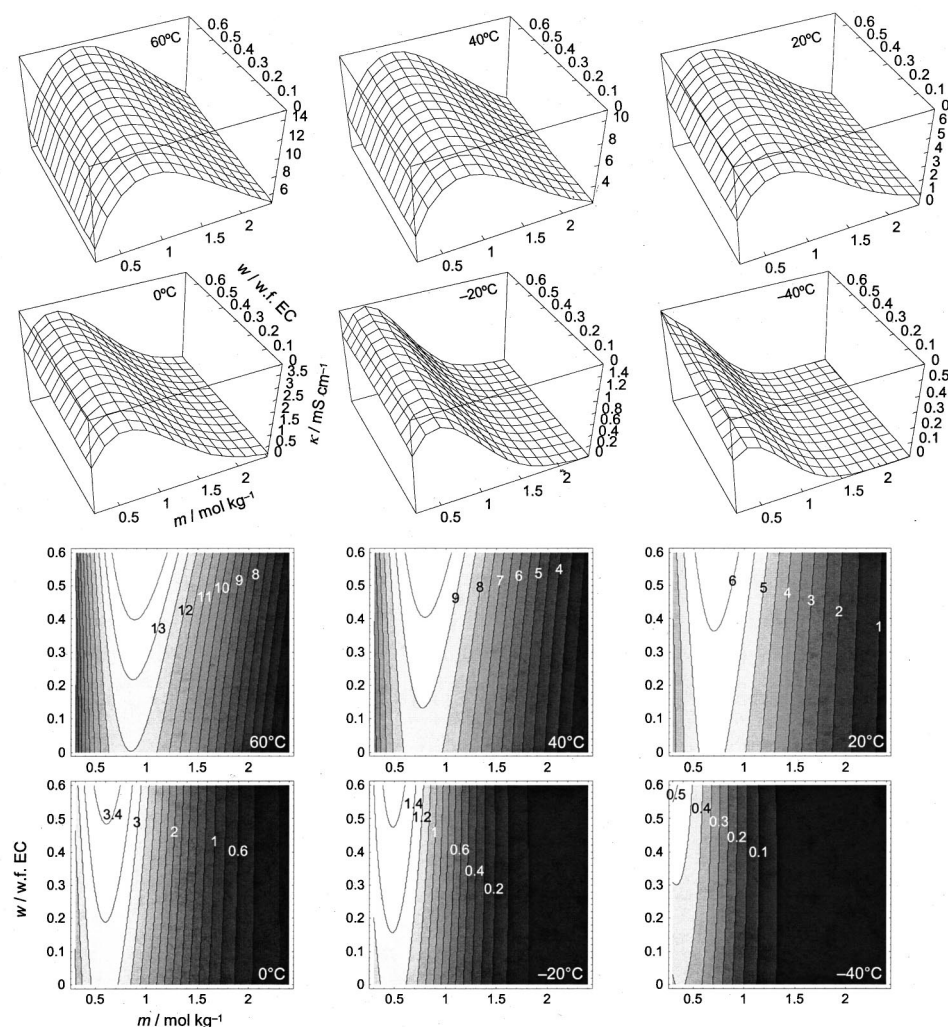


Figure 6. Change of conductivity κ with simultaneous changes in salt molarity m and solvent weight fraction w for $(\text{LiPF}_6)_m\text{-PC}_{1-w}\text{EC}_w$ solution according to the fitting functions listed in Table II. Each function is doubly represented by a surface plot (upper plots) and a contour plot (lower plots) with the set temperature and the contour values indicated in the plots.

lytes, reflecting the process of κ first increasing with the effective molarity m_e as m increases and then falling as the rise of η and fall of m_e due to ion association become dominant; this has been observed for many electrolytes of lithium salts.^{13,15-19} Peaking of κ in w seems to be the result of both the ε and η of DEC being much lower than those of PC and both being monotonic functions of w as we have learned. As such, as w rises from zero, the change of κ is first dominated by the fall of η of the electrolyte causing κ to rise and then by the fall of ε of the solvent which lowers m_e by ion association and causes κ to fall. (Exceptions have been found in DOL-DME and DOL-THF solutions of LiBF_4 , DOL, DME, and THF being 1,3-dioxolane, 1,2-dimethoxyethane, and tetrahydrofuran, respectively, of which the κ reached a maximum with DOL content in the solvent even though DOL had a higher η and lower ε than either DME or THF.⁹) The same behavior has been observed in $\text{LiPF}_6\text{-(EC-EMC)}$ ⁵ where EMC has a much lower ε and η than EC, and in $\text{LiClO}_4\text{-(PC-DME)}$ ²⁰ and $\text{NaClO}_4\text{-(PC-DME)}$,¹⁰ where DME has a much lower ε and η than PC.

Another feature of Fig. 5 is the shifting of the κ dome in the direction of low m and high w as θ lowers. This is the result of θ affecting the dome-forming process discussed above. As η rises with lowering θ , the peaking of κ with rising m occurs earlier as the higher η helps to offset the increase in m_e . Likewise, the peaking of κ with rising w occurs later as the higher η delays the dominance of a falling m_e over a falling η . The rapid rise of η with falling θ also explains the general fall in height of the domes shown in Fig. 5. In addition, as θ lowers, the dome becomes narrower in the direction of

m , indicating an increase in the rate with which η rises with m at lower θ . All these features have been observed in $\text{LiPF}_6\text{-(EC-EMC)}$ solution as described in a previous paper.⁵

PC-EC solution of LiPF_6 .—Figure 6 plots the fitting functions of Table II as the κ surfaces for $(\text{LiPF}_6)_m\text{-PC}_{1-w}\text{EC}_w$ solution in the same way as Fig. 5 did for $(\text{LiPF}_6)_m\text{-PC}_{1-w}\text{DEC}_w$. Compared to the latter, the κ surfaces here assume the shape of an “arch” instead of a dome, κ peaking only in m but rising continuously with w . This is because compared to PC, EC has a considerably higher ε but only a slightly higher η . Thus, as w increases, ε of the solvent rises but η of the electrolyte remains very much the same, resulting in the constant dominance of a rising m_e that causes the continuous rise in κ . The same dependency of κ on w , in a more accentuated fashion, has been observed in $(\text{LiPF}_6)_m\text{-(EC}_{0.3}\text{PC}_{0.3}\text{EMC}_{0.4})_{1-w}\text{TFP}_w$ solution, where tris(2,2,2-trifluoroethyl) phosphate (TFP) has a considerably higher η and a lower ε than $\text{EC}_{0.3}\text{PC}_{0.3}\text{EMC}_{0.4}$, which causes the κ of the solution to fall quickly and linearly with w .⁴ Apart from the arch shape as opposed to the dome shape, other features in the κ surfaces of Fig. 6 can all find their counterparts in Fig. 5, with the same underlying mechanisms and explanations.

Comparison of the PC-DEC and PC-EC solutions.—To observe and compare the effects of the DEC and EC content on the κ of the two solutions more quantitatively, in Fig. 7 are plotted the ratios of κ of $(\text{LiPF}_6)_m\text{-PC}_{1-w}\text{DEC}_w$ and of $(\text{LiPF}_6)_m\text{-PC}_{1-w}\text{EC}_w$ over the κ of $(\text{LiPF}_6)_m\text{-PC}$. Comparison of the two columns of plot for the two

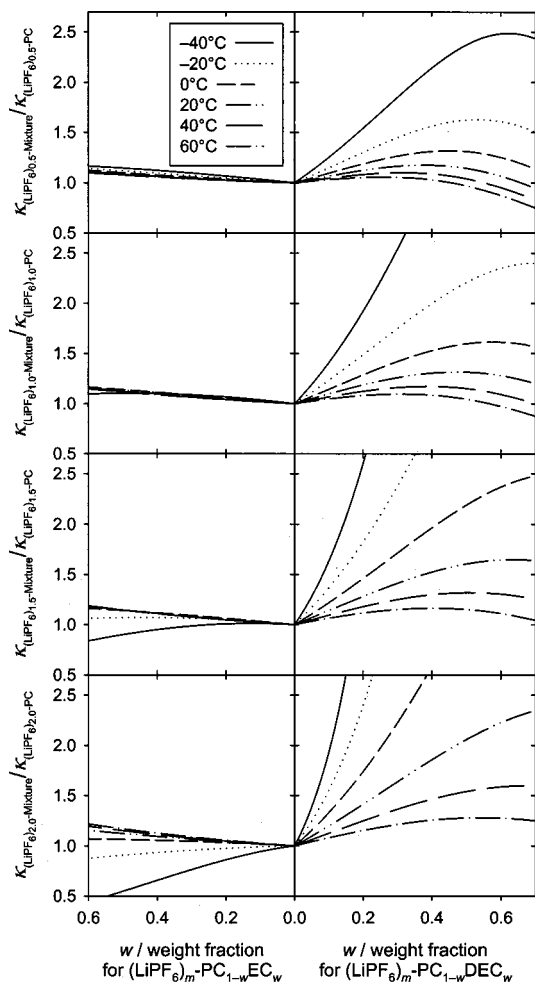


Figure 7. Change of conductivity κ with solvent weight fraction w of DEC and EC for $(\text{LiPF}_6)_m\text{-PC}_{1-w}\text{DEC}_w$ and $(\text{LiPF}_6)_m\text{-PC}_{1-w}\text{EC}_w$ solutions at different temperatures for four different salt molalities as indicated in the plots. The ordinate values of these plots are ratios of the conductivity of $(\text{LiPF}_6)_m\text{-PC}_{1-w}\text{DEC}_w$ (right column) or of $(\text{LiPF}_6)_m\text{-PC}_{1-w}\text{EC}_w$ (left column) over that of $(\text{LiPF}_6)_m\text{-PC}$.

solutions shows that the variation in κ with w is much greater for $(\text{LiPF}_6)_m\text{-PC}_{1-w}\text{DEC}_w$ than for $(\text{LiPF}_6)_m\text{-PC}_{1-w}\text{EC}_w$, as a result of PC having an η much higher than DEC but only slightly lower than EC as discussed previously. This also explains the need for a higher degree in the polynomial of Eq. 4 than of Eq. 5. The strong effect of θ on the dependency of κ on w can be seen in the right column for $(\text{LiPF}_6)_m\text{-PC}_{1-w}\text{DEC}_w$. For instance, at 1.0 m, κ rises from that of $(\text{LiPF}_6)_m\text{-PC}$ by 25% at its peak point of 0.5 of w at 20°C, 60% at 0.6 at 0°C, 140% at 0.7 at -20°C, and 400% at 0.8 at -40°C (off the plot). This trend continues and becomes more pronounced at higher m as shown in the lower plots. It thus shows clearly the effectiveness of a little relief from a high- η situation in raising the κ of an electrolyte of a high m at low θ , and thereby the importance of having a significant amount of a low- η component in the electrolyte for low temperature applications. The shifting out of the peak points with lower θ reflects the increasing difficulty of dominating a rising η by a lowering ε , which also explains the same shifting-out with a rising m from top plot to bottom plot.

The same change in the plots of the left column for $(\text{LiPF}_6)_m\text{-PC}_{1-w}\text{EC}_w$ is much milder, with the continuous rise of κ with w demonstrating the overwhelming dominance of change of ε over η and with the almost overlapping curves for different θ demonstrating the temperature independence of m_e or ion association

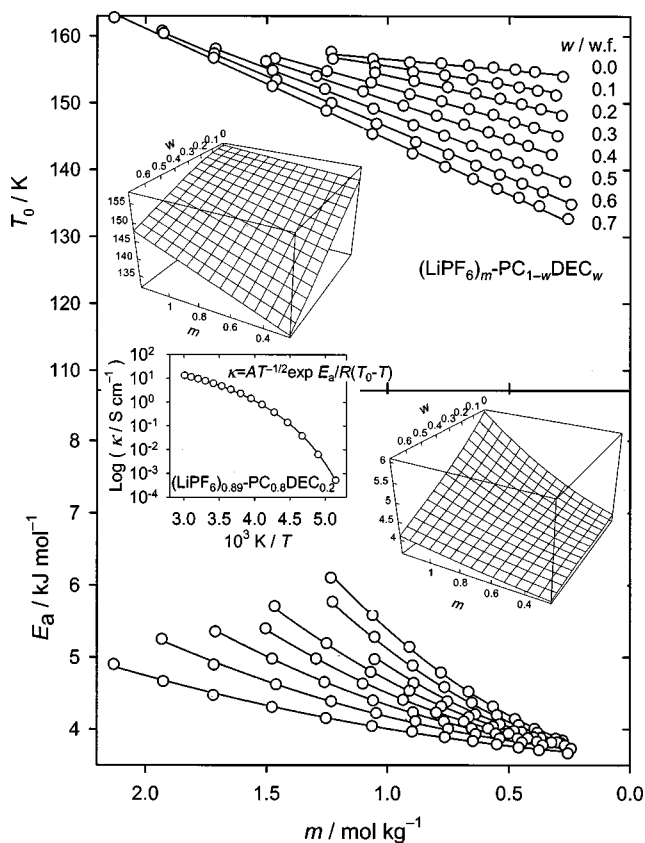


Figure 8. Results of fitting the $\ln \kappa$ - T data with the VTF equation of Eq. 6 for $(\text{LiPF}_6)_m\text{-PC}_{1-w}\text{DEC}_w$ solution at different salt molalities m and solvent weight fractions w . The upper and the lower plots describe, respectively, the vanishing mobility temperature T_0 and the apparent activation energy E_a , with (○) representing the results from fitting Eq. 6 and the curves and the surfaces representing the polynomial functions of Eq. 7 and 8 obtained from fitting the data of the open circles.

with θ . This latter observation is in full agreement with the result obtained in a previous study³ that the degree of ion association for the solvent systems PC-DEC and PC-EC, based on the Bjerrum model, did not change appreciably with θ . The increasingly apparent change of the κ - w curve with θ at higher m is due to the limited difference in η between EC and PC being magnified by the high- η environment: the higher η of EC in those concentrated electrolytes becomes dominant over ε at lower θ causing the κ to fall with w instead of to rise.

Fitting κ - T data with VTF equation for PC-DEC solution of LiPF_6 .—When the κ - T data measured for electrolytes of LiPF_6 -MOEMC-EC (MOEMC: 2-methoxyethyl methyl carbonate) were fitted with VTF equation, the vanishing mobility temperature T_0 (also called theoretical glass transition temperature) rose with salt concentration and differed from T_g by only a few degrees.^{21,22} Similarly for electrolytes of $(\text{LiPF}_6)_m\text{-(EC}_{0.3}\text{PC}_{0.3}\text{EMC}_{0.4})_{1-w}\text{TFP}_w$ ⁴ and $(\text{LiPF}_6)_m\text{-EMC}_{1-w}\text{EC}_w$,⁵ T_0 depended on m and w the same way as T_g but lower in value than T_g by a few degrees at the closest approach. One reason for the unusual closeness was suggested to be that the values of T_g of the electrolytes were too far below the temperatures at which the fitting data were measured, which was limited to -30°C by crystallization of EC.^{4,5} The $(\text{LiPF}_6)_m\text{-PC}_{1-w}\text{DEC}_w$ solution of this study, being strongly resistant to crystallization, enabled its κ to be measured down to -80°C, the limit of the temperature control mechanism of the environmental chamber. This limit was on average only 27°C higher than T_g of the

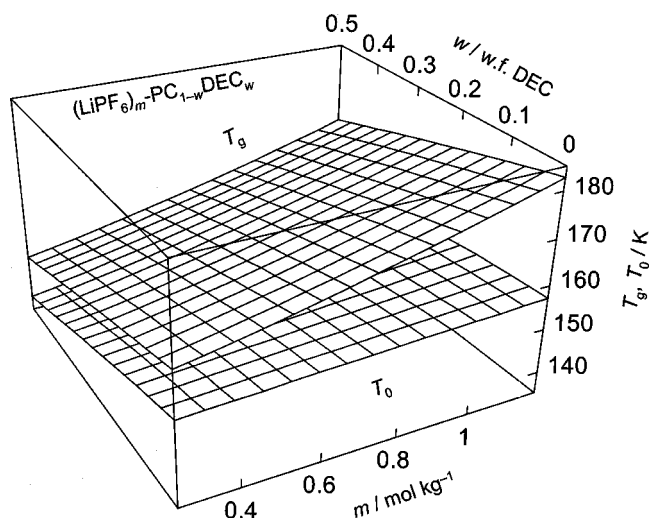


Figure 9. Comparison of T_g and T_0 surfaces as, respectively, represented by Eq. 1 and 7 in the coordinates of salt molality m and solvent weight fraction w for $(\text{LiPF}_6)_m\text{-PC}_{1-w}\text{-DEC}_w$ solution.

samples, the closest being only 10°C. Its κ - T data in the range of 60 to -80°C therefore were fit with the VTF equation

$$\ln \kappa = A - \frac{1}{2} \ln T - \frac{E_a}{R(T - T_0)} \quad [6]$$

where A , E_a , and T_0 are the three fitting parameters with E_a as the apparent activation energy.^{9,23-26} The VTF equation was used in its logarithmic form in Eq. 6 to fit the $\ln \kappa$ - T data to avoid fits that would favor data of higher T more strongly than data of lower T , as a result of the much smaller values of κ of the latter than of the former in the wide temperature range. Fitting results of acceptable consistency for T_0 and E_a are shown in Fig. 8, with an average fitting error of 0.40% of the range of the fitting data. An example of the fit for an electrolyte of $(\text{LiPF}_6)_{0.89}\text{-PC}_{0.8}\text{-DEC}_{0.2}$ is plotted in the inset. These fitting values as plotted with the open circles in Fig. 8 were further fit with polynomial functions, which are also plotted in the figure with the curves and the 3D surfaces. These polynomials are for T_0 and E_a in the upper and lower plots, respectively

$$T_0 = 153.28 + 3.2666m - 32.917w + 25.168mw - 17.994w^2 - 8.8405mw^2 + 19.189w^3 \quad [7]$$

where T_0 is in kelvin, the application limits are 0.25 to 1.3 mol kg⁻¹ for m and 0 to 0.7 weight fraction for w , and the fitting error is 0.71% of the range of the fitting data, and

$$E_a = 3.5973 + 0.60194m + 1.1876m^2 + 0.016954w - 1.5101mw - 1.4451m^2w + 1.0814w^2 + 1.3619mw^2 - 1.521w^3 \quad [8]$$

where E_a is in the unit of kJ mol⁻¹, the application limits are the same as those of Eq. 7, and the fitting error is 0.65% of the range of the fitting data.

The 3D surface of T_0 in the upper plot of Fig. 8 shows T_0 to be a simple surface slanting down from the high- η corner of high m and low w to the low- η corner of low m and high w , like that of T_g shown in Fig. 1. This is expected considering the close connection between T_g and T_0 , and has been observed in other electrolyte systems.^{4,5,25,27} Furthermore, T_0 now lies below T_g by a considerably larger distance than in the other systems,^{4,5} as can be seen from Fig. 9 where the T_g surface of Fig. 1 and the T_0 surface of Fig. 8

have been plotted together. This distance is about 30° at higher m and lower w and more than 10° at lower m and higher w . The surface plot for the apparent activation energy E_a , shown in the lower plot of Fig. 8, describes another simple surface slanting up from the low- η to the high- η corner, indicating the association of a higher E_a with a higher η . These behaviors of the T_0 and E_a derived here from κ - T data are entirely consistent with those of the same parameters derived from η - T data for many liquids, indicating in the electrolytes of this study a low degree of decoupling between the motion of ion and of solvent body or a high degree of assistance the solvent molecules provide to the ion transport.^{21,22} In addition, judging from the flattening of the E_a surface toward the low- η corner, it is unlikely that a negative E_a ever results for an electrolyte of this system, as has been reported for certain low- η electrolytes.⁹ For comparison, E_a has been evaluated to range from 4.2 to 4.8 kJ mol⁻¹ for some low- η electrolytes⁹ and from 5.5 to 9.4 kJ mol⁻¹ for some low-melting molten salts.²⁶

Conclusions

Glass transition temperature T_g of PC-DEC and PC-EC solutions of LiPF_6 rose with the salt molality m and fell with the weight fraction w of DEC but rose with w of EC in the solvents, the effects of m and w being independent of each other. This change of T_g was believed to reflect a parallel change in the viscosity η of the solutions. Conductivity κ of the PC-DEC solution of LiPF_6 , in its change with m and w at different temperatures θ , peaked in both variables and thus formed a dome when plotted as a 3D surface in the mw coordinates, while κ of the PC-EC solution peaked only in m thus assuming an arch-shaped surface. This dome-arch difference was primarily due to PC having a dielectric constant ϵ much higher than DEC but considerably lower than EC, and a viscosity η much higher than DEC but only slightly lower than EC. In addition, as θ was lowered, the κ surfaces fell in height and shifted in the direction of low η . All these observations were the results of the interplay of ϵ of the solvents and η of the electrolytes at different values of m , w , and θ . The effects of DEC and EC on the κ of PC solution of LiPF_6 demonstrated the benefit of having a low- η solvent component in an electrolyte for it to have a decent κ at low θ and the independence on θ of ion association in these electrolytes. Fitting a VTF equation for the PC-DEC solution of LiPF_6 to its κ - T data measured down to temperatures very close to its values of T_g resulted in a reliable evaluation of its vanishing mobility temperature T_0 and its apparent activation energy E_a , both forming simple surfaces in the mw coordinates slanting up in the direction of high η . Further, the T_0 surface had the same orientation as the T_g surface in the mw coordinates, and was below the latter by more than ten degrees.

The Army Research Laboratory assisted in meeting the publication costs of this article.

References

1. I. Mills, T. Cvitas, K. Homann, N. Kallay, and K. Kuchitsu, *Quantities, Units and Symbols in Physical Chemistry*, 2nd ed., p. 48, IUPAC and Blackwell Scientific Publications, London (1993).
2. M. S. Ding, *J. Electrochem. Soc.*, Submitted.
3. M. S. Ding, *J. Electrochem. Soc.*, Accepted for publication.
4. M. S. Ding, K. Xu, and T. R. Jow, *J. Electrochem. Soc.*, **149**, A1489 (2002).
5. M. S. Ding, K. Xu, S.-S. Zhang, K. Amine, G. L. Henriksen, and T. R. Jow, *J. Electrochem. Soc.*, **148**, A1196 (2001).
6. *Electrolyte Data Collection, Part 1d, Conductivities, Transference Numbers and Limiting Ionic Conductivities of Aprotic, Protophobic Solvents II. Carbonates*, J. Barthel and R. Neuder, Editors, Chemistry Data Series, Vol. XII, DECHEMA, Frankfurt (2000).
7. *Handbook of Organic Solvents*, D. R. Lide, Editor, CRC Press, Boca Raton, FL (1995).
8. G. E. Blomgren, in *Lithium Batteries*, J.-P. Gabano, Editor, Academic Press, London (1983).
9. Y. Matsuda, M. Morita, and T. Yamashita, *J. Electrochem. Soc.*, **131**, 2821 (1984).
10. Y. Matsuda and H. Satake, *J. Electrochem. Soc.*, **127**, 877 (1980).
11. J. Barthel, R. Neuder, and H. Roch, *J. Chem. Eng. Data*, **45**, 1007 (2000).

12. M. S. Ding, K. Xu, and T. R. Jow, *J. Electrochem. Soc.*, **147**, 1688 (2000).
13. A. Cisak and L. Werblan, *High-Energy Non-aqueous Batteries*, Chap. 7, Ellis Horwood, New York (1993).
14. J. F. Casteel, J. R. Angel, H. B. McNeely, and P. G. Sears, *J. Electrochem. Soc.*, **122**, 319 (1975).
15. J. F. Casteel and E. S. Amis, *J. Chem. Eng. Data*, **17**, 55 (1972).
16. J. Barthel, R. Buestrich, E. Carl, and H. J. Gores, *J. Electrochem. Soc.*, **143**, 3565 (1996).
17. J. Barthel, H. J. Gores, and G. Schmeer, *Ber. Bunsenges. Phys. Chem.*, **83**, 911 (1979).
18. Y. Choquette, G. Brisard, M. Parent, D. Brouillette, G. Perron, J. E. Desnoyers, M. Armand, D. Gravel, and N. Slougui, *J. Electrochem. Soc.*, **145**, 3500 (1998).
19. H. P. Chen, J. W. Fergus, and B. Z. Jang, *J. Electrochem. Soc.*, **147**, 399 (2000).
20. Y. Matsuda, M. Morita, and K. Kosaka, *J. Electrochem. Soc.*, **130**, 101 (1983).
21. G. Y. Gu, S. Bouvier, C. Wu, R. Laura, M. Rzeznik, and K. M. Abraham, *Electrochim. Acta*, **45**, 3127 (2000).
22. G. Y. Gu, R. Laura, and K. M. Abraham, *Electrochem. Solid-State Lett.*, **2**, 486 (1999).
23. S. I. Smedley, *The Interpretation of Ionic Conductivity in Liquids*, Chap. 3, Plenum Press, New York (1980).
24. W. Xu and C. A. Angell, *Electrochem. Solid-State Lett.*, **4**, E1 (2001).
25. J. Barthel, R. Meier, and B. E. Conway, *J. Chem. Eng. Data*, **44**, 155 (1999).
26. A. B. McEwen, H. L. Ngo, K. LeCompte, and J. L. Goldman, *J. Electrochem. Soc.*, **146**, 1687 (1999).
27. C. A. Angell and D. L. Smith, *J. Phys. Chem.*, **86**, 3845 (1982).